European Journal of Pharmaceutics and Biopharmaceutics 153 (2020) 177–186

Contents lists available at ScienceDirect

European Journal of Pharmaceutics and Biopharmaceutics

journal homepage: www.elsevier.com/locate/ejpb

Preparation and characterization of lamotrigine containing nanocapsules for nasal administration

Péter Gieszinger[a], Noemi Stefania Csaba[b], Marcos Garcia-Fuentes[b], Maruthi Prasanna[b], Róbert Gáspár[c], Anita Sztojkov-Ivanov[d], Eszter Ducza[d], Árpád Márki[e], Tamás Janáky[f], Gábor Kecskeméti[f], Gábor Katona[a], Piroska Szabó-Révész[a], Rita Ambrus[a,*]

[a] University of Szeged, Inderdisciplinary Excellence Centre, Institute of Pharmaceutical Technology and Regulatory Affairs, Eötvös u. 6., H-6720 Szeged, Hungary
[b] University of Santiago de Compostela, Center for Research in Molecular Medicine and Chronic Diseases (CiMUS), 15782 Campus Vida, Santiago de Compostela, Spain
[c] Department of Pharmacology and Pharmacotherapy, University of Szeged, Dóm tér 12, H-6720 Szeged, Hungary
[d] Department of Pharmacodynamics and Biopharmacy, University of Szeged, Eötvös u. 6, H-6720 Szeged, Hungary
[e] Department of Medical Physics and Informatics, University of Szeged, Faculty of Medicine, H-6720 Szeged, Korányi fasor 9., Hungary
[f] Department of Medical Chemistry, University of Szeged, Dóm tér 8, H-6720 Szeged, Hungary

ARTICLE INFO

Keywords:
Nanosystem
Nasal delivery
Nanocapsules
Lamotrigine
Epilepsy

ABSTRACT

Nanocapsules (NCs) have become one of the most researched nanostructured drug delivery systems due to their advantageous properties and versatility. NCs can enhance the bioavailabiliy of hydrophobic drugs by impoving their solubility and permeability. Also, they can protect these active pharmaceutical agents (APIs) from the physiological environment with preventing e.g. the enzymatic degradation. NCs can be used for many administration routes: e.g. oral, dermal, nasal and ocular formulations are exisiting in liquid and solid forms. The nose is one of the most interesting alternative drug administration route, because local, systemic and direct central nervous system (CNS) delivery can be achived; this could be utilized in the therapy of CNS diseases. Therefore, the goal of this study was to design, prepare and investigate a novel, lamotrigin containing NC formulation for nasal administration. The determination of micrometric parameters (particle size, polydispersity index, surface charge), *in vitro* (drug loading capacity, release and permeability investigations) and *in vivo* characterization of the formulations were performed in the study. The results indicate that the formulation could be a promising alternative of lamotrigine (LAM) as the NCs were around 305 nm size with high encapsulation efficiency (58.44%). Moreover, the LAM showed rapid and high release from the NCs *in vitro* and considerable penetration to the brain tissues was observed during the *in vivo* study.

1. Introduction

In the last decade, encapsulation of Active Pharmaceutical Ingredients (APIs) has become increasingly important due to its advantages over traditional technological methods for solubilization (e.g. solid dispersions, ammorphization). Indeed, some nanocarriers can improve the solubility of hydrophobic drugs and thereby enhance their bioavailability [1–3]. Nanocapsules (NCs) consist of an oily core and a biodegradable polymer shell. This structure can protect the APIs from the physiological environment (e.g. pH, enzymatic degradation) and enhance their permeability through biological barriers [4–8]. Further advantages are that the NCs can reduce drug toxicity and increase their stability. NCs have been developed for different administration routes. Among these routes the oral and the parenteral routes are the most researched, but there have been some efforts to prepare dermal, ocular or nasal formulations [9–19].

Nasal delivery is an alternative route for drug administration and has become increasingly investigated in the last years. Via the nasal route drugs can be delivered locally, systemically, but also directly into the central nervous system (CNS), which is the unique property of nasal administration. This is a barely understood mechanism for the direct transport of drugs from nose-to-brain that overcomes the blood-brain-

* Corresponding author at: University of Szeged, Institute of Pharmaceutical Technology and Regulatory Affairs, Eötvös u. 6., H-6720 Szeged, Hungary.
E-mail addresses: noemi.csaba@usc.es (N. Stefania Csaba), marcos.garcia@usc.es (M. Garcia-Fuentes), gaspar@med.u-szeged.hu (R. Gáspár), Ivanov.Anita@pharm.u-szeged.hu (A. Sztojkov-Ivanov), ducza@pharm.u-szeged.hu (E. Ducza), marki.arpad@med.u-szeged.hu (Á. Márki), janaky.tamas@med.u-szeged.hu (T. Janáky), kecskemeti.gabor@med.u-szeged.hu (G. Kecskeméti), katona@pharm.u-szeged.hu (G. Katona), revesz@pharm.u-szeged.hu (P. Szabó-Révész), arita@pharm.u-szeged.hu (R. Ambrus).

https://doi.org/10.1016/j.ejpb.2020.06.003
Received 31 January 2020; Received in revised form 12 May 2020; Accepted 7 June 2020
Available online 10 June 2020
0939-6411/

barrier (BBB) [15–25]. Therefore, in the case of CNS diseases, the nasal route can be an attractive way to deliver APIs directly into the CNS by a non-invasive way [26–34]. Other advantages are that the administration for nose-to-brain delivery is not painful and sterility is not a formulation requirement [26,35]. In the literature some articles could be found, where e.g. statin or benziodiazepine containing NCs were investigated via nasal route [36–38]. In these studies the researchers aimed to develop and investigate these formulations *in vivo* and the APIs presented in the brain tissues after nasal administration of NCs, so they could be suitable for the treatment of other diseases.

Lamotrigine (LAM) is a poorly water soluble, second generation antielpileptic drug from the phenyltriazine class, that is currently available only in tablet form [39–43]. It has been applied in many *in vivo* studies, but there the aims were to evaluate its immunmodulatory effect [44,45], bioactivation [46], formulation of gastroretentive matrix tablets, chewable/dispersible tablets [47,48] or iv. nanoformaultion [41]. Also, there was a study, in which LAM was used intranasally, but there the goal was to determine the phamarcokinetic properties of the API [34].

Our research group has made successful efforts to develop nasal powder form of LAM with a top-down method [49,50]. As the nose is a great alternative administration route to allocate APIs directly into the CNS and provides great possibilty to take advantage of NCs, we envisage that a novel, NC formulation made with a bottom-up method could improve the interaction between the drug and the nasal epithelium. Thus the advantages of the nasal delivery and NCs could be combined [19,51–53]. Therefore, the aims of this study were to design and prepare LAM-loaded chitosan NC formulations for nasal drug delivery. For this, we optimized the preparation method of the formulations, we characterized the NCs properties and studied their delivery performance under *in vitro* and *in vivo* conditions.

2. Materials and methods

2.1. Identification of factors affecting product quality

Quality by Design (QbD) is a holistic and systematic quality management technique, where the development design is knowledge and based; thus, the experiments can be planned more efficiently and economically. As part of the QbD methodology, an Ishikawa diagram was set up to identify a knowledge space of the NCs. With the Ishikawa diagram, the identification and systematization of influencing factors were carried out. The factors with the highest influence were chosen and varied [49,54].

2.2. Materials

LAM, was purchased from Teva Ltd. (Budapest, Hungary). Glyceryl monooleate (Type 40) (Peceol®) and Diethylene glycol monoethyl ether (Transcutol HP®) were a kind gift from Gattefossé (St. Preist, France). Polyoxyetylene (40) monostearate (PEG-stearate 40) was purchased from Croda (East Yorkshire, United Kingdom). Chitosan hydrochloride salt was obtained from HMC+ (Halle, Germany). Mannitol was obtained from Sigma-Aldrich (New York, USA).

2.3. Methods

2.3.1. Preparation of nanocapsules (NCs)

The NCs were prepared by a solvent displacement method, whose compositition (Table 1) was optimized after preliminary experiments. The liquid lipid: surfactant ratio was varied on 3 levels (2:1, 1:1 and 1:2), of which the 1:1 ratio showed proper in terms of particle size, PDI and surface charge. In this sample, the organic phase was first prepared by adding the adeaquate amount of LAM solution (100 mg/mL DMSO solution), Peceol® and Transcutol® to PEG-stearate 40 solution (5.33 mg/mL ethanol solution). Then, this solution was poured over 2 mL of ultrapure water under continous magnetic stirring to from an o/w emulsion. After 10 min, 2 mL of chitosan solution (1 mg/mL) was added upon this emulion under magnetic stirring, leading to the spontaneous formation of the NCs.

Table 1
The compositition of the NC formulations.

	1:1	2:1	1:2	+ 2 mL MilliQ water	+ 2 mL 1 mg/ml Chitosan solution after 10 mins
LAM solution(100 mg/ml) (μL)	100	100	100		
Peceol® (μL)	41.7	83.4	41.7		
Transcutol®(μL)	41.7	41.7	83.4		
PEG-stearate 40 solution (5.33 mg/mL EtOH solution)	816.6	774.9	774.9		

After 10 additional minutes of stirring, the NCs were isolated and concentrated to a final theoretical chitosan concentration of 1 mg/ml by centrifugation (Hettich Universal 32 R; Tuttlingen, Germany) at 33000xg for 33 min at 15 °C. In parallel, control blank NCs, without LAM were prepared using the same method.

2.3.2. Preparation of freeze-dried nanocapsules (FDNCs)

The freeze-drying was performed in Scanvac CoolSafe 100-9 Pro type equipment (LaboGene ApS, Lynge, Denmark) equipped with a 3-shelf sample holder unit, recessed into the drying chamber. The prepared NCs were lyophilized with 5% mannitol. The process was controlled by a computer program (Scanlaf CTS16a02), the temperature and pressure values were recorded continuously. In the first period of the freeze-drying the chamber was cooled from room temperature to −25 °C. At this time the vacuum was turned on (p = 0,013 mBar). Then the samples were kept under these conditions for 12 h, whileafter during the secondary drying the temperature was raised up to +25 °C. temperature. The secondary drying lasted for 4 h to produces the final solid phase prodcuts (FDNCs). Fig. 1. illustrates the process of the NC preparation.

2.3.3. Particle size, particle size distribution and surface charge characterization of NCs

The particle size and polydispersity index of the NCs were determined by photon correlation spectroscopy (PCS) (Zetasizer NanoZS®, Malvern Instruments; Malvern, United Kingdom). In the case of surface charge, zeta potential (ZP) measurements were done by laser Doppler anemometry (LDA) using the same equipment. All the measurements were performed at 25 °C with a detection angle of 173° in distilled water, unless otherwise indicated. The freeze-dried NCs were investigated with the same instrument after redispergation with MilliQ water. The FDNCs samples were investigated after resuspension in MilliQ water.

2.3.4. Encapsulation efficacy (EE) and drug loading (DL)

After centrifugation the supernatant was analyzed for the amount of drug present with a UV spectrophotometer (SynergyTM H1 Microplate Reader, BioTek Instruments, Inc.) at λ_{max} of 307 nm after suitable dilution. EE% was calculated by the following equation:

The calculation of encapsulation efficacy

$$\%EE = ((W_1 - W_2)/W_1)\frac{W_1 - W_2}{W_2} * 100 \quad (1)$$

Loading capacity (percentage drug loading [%DL]) was calculated by the following equation:

The calculation of percentage of drug loading

$$\%DL = ((W_1 - W_2)/(W_1 - W_2 + W_{lipid}))\frac{W_1 - W_2}{W_2} * 100 \quad (2)$$

where, W_1, W_2 and W_{lipid} are the weight of drug added in the

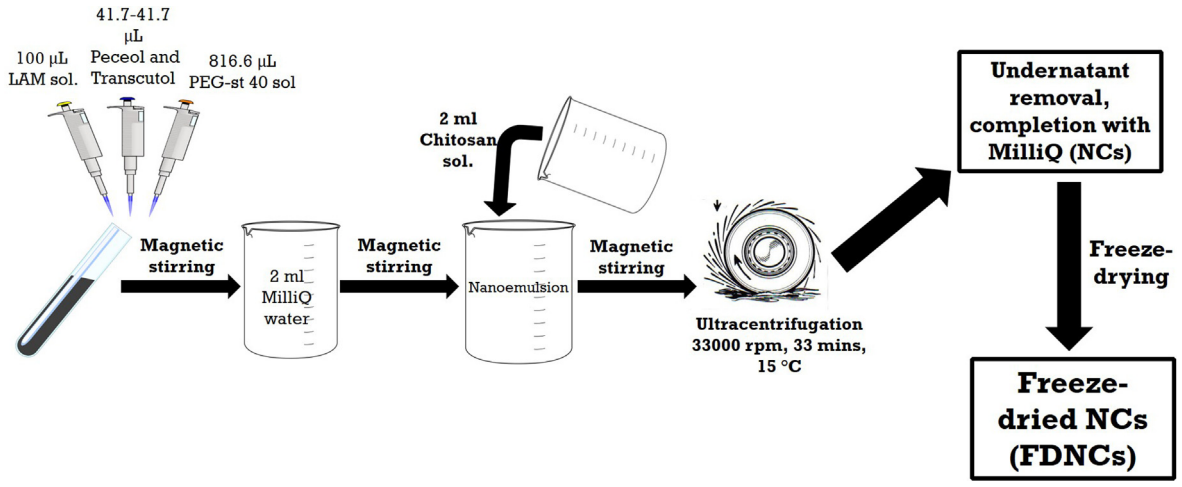

Fig. 1. The process of LPNC and SPNC preparation.

formulation, analyzed weight of drug in supernatant and weight of lipid added in formulation, respectively.

2.3.5. Morphology of NCs

For the SEM investigation, NC formulation were diluted and dried. The morphology of NCs was investigated by SEM (Hitachi S4700; Hitachi Ltd., Tokyo, Japan) at 10 kV. The samples were gold–palladium coated (90 s) with a sputter coater (Bio- Rad SC502; VG Microtech, Uckfield, UK) using an electric potential of 2.0 kV at 10 mA for 10 min. The air pressure was 1.3–13.0 mPa. To confirm the particle size measurements obtained by PCS (Section 2.3.5), the size of the freeze-dried NCs were obtained by analyzing SEM images with the ImageJ software (1.50i; Java 1.6.0_20 [32-bit]; Windows NT) using approximately 500 particles.

2.3.6. In vitro drug release study

The modified paddle method (USP dissolution apparatus, type II; Pharma Test, Hainburg, Germany) was used to examine the dissolution rate of LAM-containing NCs and determine the drug release profile from the samples. To model the nasal pH and temperature conditions, the medium was 9 mL phosphate-buffered saline (PBS) adjusted to pH 5.60. Samples with 1.65 mg (n = 3) LAM content were tested in this medium at 30 °C with paddle stirring at 50 rpm. The sampling points were at 5 min, 10 min, 15 min, 30 min, 45 min and 60 min. After each sampling point, the medium was made up to 9 mL. The first data points were considered the most important as the mucociliary clearance renews the mucus every 15 min. The following data points offered additional information about the dissolution behavior of LAM. The samples were investigated with a RP-HPLC-DAD system. The RP-HPLC-DAD was consisted of an Agilent 1200 Series chromatograph and a DAD detector. The statonary phase was a Kinetex® C_{18} colonna (150 mm × 4,6 mm, particle size: 5 µm, pore diameter size: 100 Å). The separation was isocratic, the composition of the mobile phase was 0,01 M phosphate buffer (pH = 6,7 ± 0,1): methanol: acetonitrile = 50:20:30 (v/v). The analytical column was tempered for 25 °C and the measurements lasted 10 mins. The flow rate was 0.75 mL/min, and 10 µL of sample was injected into the flowing fluid, measured at 307 nm. The equation for the calibration line was: $y = 12{,}335x - 3{,}488$ ($R^2 = 1$). The equation was valid in the range of 10–150 µg/ml. The tests were carried out in triplicates.

2.3.7. In vitro permeability study

The horizontal diffusion test (Side-Bi-Side™, Crown Glass, USA) was carried out under simulated nasal conditions (pH 5.6, 30 °C). The tested samples (n = 3) contained 1.65 mg LAM. The cellulose ester membrane with 0.45 µm pore diameter was soaked in isopropyl myristate 30 min before the investigation, and the donor phase was tempered to 30 °C at pH 5.6. The powder samples were washed into the chamber with the medium of the donor phase in the beginning of the study. The acceptor phase was at pH 7.4, and the concentration of diffused API was measured spectrophotometrically in real time at 307 nm with an AvaLight DH-S-BAL spectrophotometer (AVANTES, Netherlands) connected to an AvaSpec-2048L transmission immersion probe (AVANTES, Netherland) with optical fiber. The path length was 1 cm. The tests were carried out in triplicate.

2.3.8. In vivo studies

2.3.8.1. Intranasal administration, blood sample collection, and brain removal. The NC formulation contained 0.066 mg LAM, while the FDNCs formulation contained 0.039 mg LAM. These were the maximum doses that were able to administer to the animals. This dose was administered into the right nostril of 160–180 g male Sprague–Dawley rats (n = 4) with a small spatula. As a control, IV injections of LAM solution (IV LAM) containing 0.555 mg of API were given to rats (n = 4). The administration was carried out under isoflurane anesthesia. At predetermined time points (3, 6, 10, 20, 40 and 60 min) after LAM dosing, the blood of the rats—under deep isoflurane anesthesia—was collected into heparinized tubes by cardiac puncture. Then the animals were sacrificed by decapitation and brain tissues were quickly removed, rinsed in ice-cold PBS, divided into left and right hemispheres, weighed, and stored at −80 °C until assayed. The experiments were performed according to the EU Directive 2010/63/EU for animal experiments and were approved by the Hungarian Ethical Committee for Animal Research (permission number: IV/1247/2017).

2.3.8.2. Plasma sample preparation. To 100 µL of plasma samples 20 µL internal standard solution (0.4 µg/mL, lamotrigine-13C3, d3 in methanol-water, 50:50, v/v), 20 µL methanol-water mixture (50:50, v/v) and 100 µL 2 M sodium hydroxide were pipetted, and the samples were vortexed. For the liquid-liquid extraction 1 mL ethyl acetate was added to each tube and vortexed for 1 min, shaken at room temperature for 10 min and left on ice for 5 min. After centrifugation, 300 µL of the supernatant was transferred to a 1.5 mL glass vial, and evaporated to dryness at room temperature using a gentle stream of nitrogen. The samples were resuspended in 50 µL of acetonitrile containing formic acid (0.1% v/v) and diluted with 0.1% formic acid to a final volume of 400 µL. 20 µL was injected into the LC-MS/MS system for analysis.

Prior to the extraction of the calibration and quality control samples, 20 µL of a standard solution (6.25 ng/ mL − 8 µg/ mL LAM) was added to LAM-free pooled rat plasma instead of methanol-water mixture. The rest of the sample preparation steps were the same as

described above.

2.3.8.3. Brain tissue sample preparation. Brain samples were homogenized in water (4 mL/g wet tissue weight) on ice 2 times for 30 s with an ULTRA-TURRAX blade-type homogenizer (IKA® Works, Inc; Wilmington, USA) and for 30 s with a BioLogics Model 150VT ultrasonic homogenizer (BioLogics Inc, Manassas, USA). The samples thus prepared were stored at −80 °C until use. On the day of extraction the samples were thawed, and to 200 µL brain homogenates 20 µL internal standard solution (0.5 µg/mL, lamotrigine-13C3, d3 in methanol-water, 50:50, v/v), 20 µL methanol-water mixture (50:50, v/v) and 20 µL 20% (w/v) trichloroacetic acid (TCA) were added. Samples were vortexed and centrifuged with 10,000 × g at 20 °C for 10 min and then 100 µL of the supernatant was placed to a new test tube. LAM was extracted after adding 100 µL 4 M sodium hydroxide and 1 mL ethyl acetate, by vortexing for 1 min, shaking at room temperature for 10 min and resting on ice for 5 min. After centifugation, 700 µL of the supernatant was transferred to a 1.5 mL glass vial then evaporated to dryness at room temperature. The samples were resuspended in 50 µL of acetonitril containing formic acid (0.1% v/v), diluted with 0.1% formic acid to a final volume of 370 µL and than 20 µL was injected into the LC-MS/MS system for analysis.

Prior to the extraction of the calibration and quality control samples, 20 µL of a standard solution (7.8125 ng/mL − 10 µg/ mL LAM) was added to the pooled LAM-free rat brain homogenate instead of methanol-water mixture. Further sample preparation steps were the same as described above.

2.3.8.4. LC-MS/MS. The liquid chromatographic separation was performed on an Agilent 1100 Series HPLC system (Agilent; Santa Clara, USA) using a Kinetex C18 (2.6 µm 100A, 50 × 2.1 mm) column (Phenomenex; Torrance, USA). In front of the analytical column, a C18 guard column was used. Water (A) and acetonitril (B) both containing formic acid (0.1% v/v) were used as mobil phases. A gradient elution program was used to elute components: gradient started at 13% B, increased linearly to 90% B in 3 min, kept at 90% B for 2 min, dropped back to 13% B in 0.1 min and kept at 13% B for 2.9 min. The flow rate was set at 300 µL/min for the separation and 500 µL/min to wash and equilibrate the column. The autosampler and the column were maintained at room temperature.

Samples were analyzed with an on-line connected Q Exactive Plus quadrupole-orbitrap hybrid mass spectrometer (Thermo Fisher Scientific; Waltham, USA) equipped with a heated electrospray ion-source (HESI). It operated in positive mode with the following conditions: capillary temperature 256 °C, S-Lens RF level 50, spray voltage 3.5 kV, sheath gas flow 48, sweep gas flow 2 and auxiliary gas flow 11. Automatic gain control (AGC) setting was defined as 2×10^5 charges and the maximum injection time was set to 100 ms. Collision energy (CE) was optimized and set at 31 eV for LAM and lamotrigine-13C3, d3 (ISTD). The precursor to product ion transition of *m/z* 256.01 → 108.98 (qualifier), 256.01 → 210.98 (quantifier) for LAM, and *m/z* 262.04 → 110.99 (qualifier), 262.04 → 217.01 (quantifier) for ISTD were used for parallel reaction monitoring (PRM).

Data acquisition and processing were performed using Xcalibur™ and Quan Browser softwares (Thermo Fisher Scientific; Waltham, USA).

2.3.8.5. Calculation of drug targeting efficiency. Drug targeting efficiency (DTE) – relative exposure of the brain to the drug following intranasal administration vs. systemic administration – was calculated according to the following formula (Eq. (3)):

The calculation of DTE values

$$DTE = \frac{\left(\frac{AUCbrain}{AUCblood}\right)IN}{\left(\frac{AUCbrain}{AUCblood}\right)IV} \quad (3)$$

The value of DTE can range from $-\infty$ to ∞, and the values higher than 1.0 indicate more efficient drug delivery to the brain following intranasal administration as compared to the systemic administration [55].

2.3.8.6. Calculations of the area under the time-concentration curve (AUC) and statistical analysis. The calculation of area under the curve (AUC) of the time (min) – concentration (µg/L) curves of each group of animals were performed with the PKSolver add-in from Microsoft Excel (MS Office 2010) using the non-compartmental analysis of data after extravascular input (model #101) of LAM [56]. The AUC values were calculated using the lineartrapezoidal method. Because of the incomplete elimination of LAM, the following parameters were not determined: λ, $t_{1/2}$, $AUC_{0\text{-inf}}$, $AUMC_{0\text{-inf}}$, V_d, and Cl. All reported data are means ± SD.

3. Results and discussion

3.1. Identification of factors affecting product quality

The first step before the experiment was to identify and systematize the most influencing factors that could affect product quality. This scheme allowed us to design our research plan more effectively, optimizing costs and time. In the Ishikawa-diagram of the NC product we could identify 4 main groups of influencing factors (Fig. 2): material characteristics, production method, investigation methods and, therapeutical and regulatory expectations. Among these factors the type and amount of surfactant, liquid lipid, surface modifier, coating material and cryoprotectant, the amount of API and the particle size, its PDI and the surface characteristics (ZP) of the NCs have the greatest impact on the quality of the product. The rest of the factors were not found to be as influencing during the preformulation tests and the literature review. After setting up the Ishikawa-diagram we decided to set up a factorial experimental plan, where the type of the coating material and the lipid was varied. The experiments were optimized for particle size and PDI.

3.2. Particle size, particle size distribution and surface charge characterization of NCs

As a first step, the particle size and surface charge of the NCs were analyzed (Fig. 2). The NCs were always in the 290–380 nm range that is acceptable according to the FDA regulatory, as the particle size of nanosystems have to be between 100 and 1000 nm [57]. Our aim was to develop NCs that were in the lower part of this range and showed homogenous particle size population (PDI < 0.2). These requirements were fulfilled for the NCs only if the liquid lipid: surfactant ratio was 1:1. LAM incorporation resulted in a significant increase in particle size compared to blank NCs. In all cases, zeta potential values were similar, positive and close to zero that may be advantageous for mucoadhesion and mucodiffusion [58]. In the other samples the particle size and PDI did not meet the criterias that we had set previously and the particles were not in the nanorange, so thereafter the most promising sample was tested.

The freeze-dried formulation showed some increase in particle size and PDI after redispergation (504 ± 3 nm, 0.538 PDI), indicating some aggregation, that could happen due to the presence of mannitol. However, this aggregation was not observed on the freeze-dried state when the powder cake was analyzed with imaging technology as the particle size showed 179 ± 62 nm. This means that the NCs maintained their size after freeze-drying. Another relevant observation was an increase in zeta potential in the NCs resuspended after freeze-drying, which can be explained by the density enhancement of chitosan that was increased due to the increase in particle size and pararelly decreased surface area. The 26.5 ± 0.9 value means that the NCs may have high degrees of stability (see Table 2).

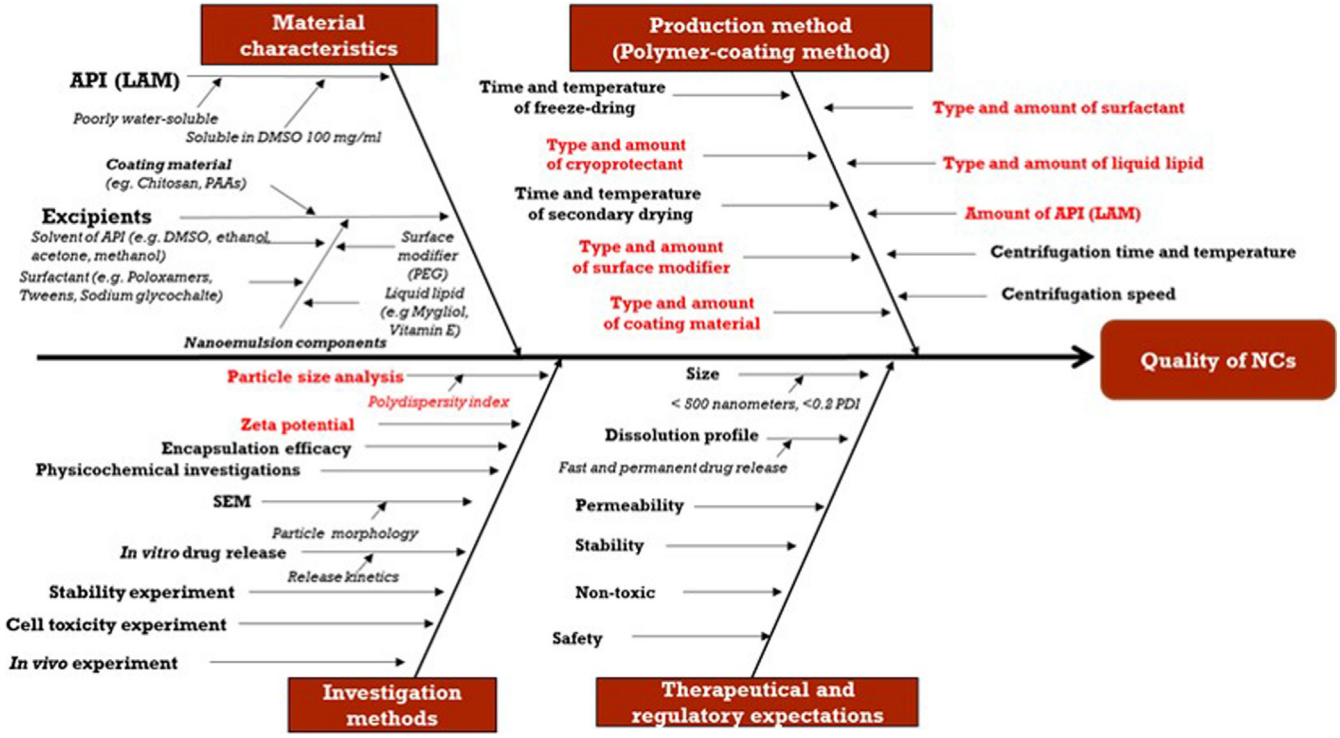

Fig. 2. Ishikawa-diagram of the NC product.

3.3. Encapsulation efficacy (EE) and drug loading (DL)

The EE of LAM was 58.44% ± 4.81 in the NCs and the DL was 5.31% ± 0.67. This is an acceptable level of EE for a nanoformulation, particularly since it was achieved with a very high drug loading. This EE means that there is 1.75 mg LAM in 1.5 mL formulation –before centrifugation– or in one dose of freeze dried cake. This is near to the lowest marketed dose and could be suitable for administration as if taken nasally, dose can be decreased.

3.4. Particle morphology

We analyzed LAM-loaded LPNCs (Fig. 3A) and freeze dried SPNCs (Fig. 3B.) by SEM. The core and shell substructures of the NCs were clearly visible before freeze drying (Fig. 3A). In both cases, NCs presented a spherical shape and homogenous distribution. There was no sign of non-encapsulated, crystalline LAM around the NCs and there was no sign of aggregation in the mannitol matrix, so the pictures indicated good particle stability and no warnings regarding drug segregation.

3.5. In vitro drug release study

The *in vitro* release study showed faster release of LAM in the case of NCs formulation compared to pure LAM powder (Fig. 4). We could detect more than 20% released LAM after 5 min and ~60% LAM after 15 min; afterwards a drug release plateau was observed. The FDNCs released the drug a slower than NCs but markedly faster than the drug powder. In this case ~40% LAM was released after 10 min, and 50% after 15 min, a point where the release started to level-off. At 15 min, both NCs formulations released between 2.5 and 3-fold more LAM than the drug powder. For nasal administration, the first four points are the most important, because the mucociliary clearance renews the nasal mucus every ~15 min, thus limiting the API residence time at this site [59,60]. In this sense, the fast release of LAM from the nanoformulations can be considered an advantageous characteristic for nasal delivery. Moreover, the use of chitosan may extend the residence time, the bioadhesion which means that the formulation could have enough time to get into the CNS and can reach enhanced absorption [24,61].

3.6. In vitro permeability study

Next, we performed a permeability study to compare how the different formulations could modify the capacity of LAM for crossing biological barriers (Fig. 5). In case of nasal administration, it is important to achieve a high permeability rate through the mucosa, which means that the API reaches its target more efficiently. NCs and FDNCs formulations performed similarly well in this experiment, and much

Table 2
Results of the particle size and surface characterization of the NCs.

	Z-average (d. nm)	PDI	Zeta potential (mV)
Blank NCs after centrifugation (2:1 ratio)	2815 ± 159	0.795	0.99 ± 0.4
LAM NCs after centrifugation (2:1 ratio)	1210 ± 68	0.773	1.3 ± 0.1
Blank NCs after centrifugation (1:2 ratio)	1477 ± 72	0.643	0.80 ± 0.3
LAM NCs after centrifugation (1:2 ratio)	1399 ± 59	0.950	0.94 ± 0.5
Blank NCs after centrifugation (1:1 ratio)	294 ± 9	0.175	0.39 ± 0.2
LAM NCs after centrifugation (1:1 ratio)	305 ± 7	0.188	1.0 ± 0.3
FDNCs	Freeze-dried: 179 ± 62 After redispergation: 504 ± 3	0.538	26.5 ± 0.9

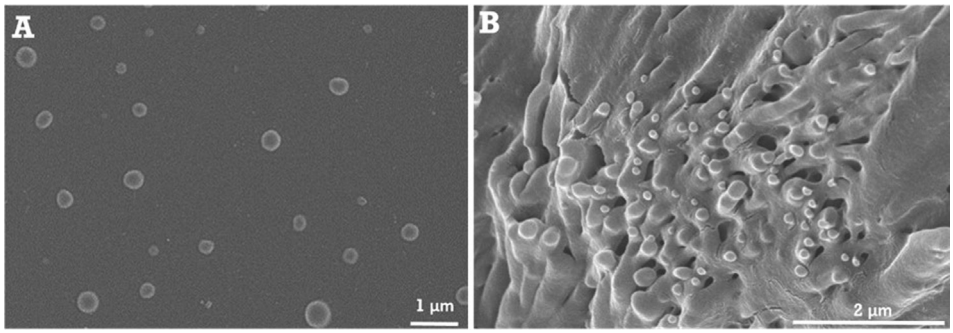

Fig. 3. The morphology of LAM loaded NCs (Picture A.) and FDNCs (Picture B.)

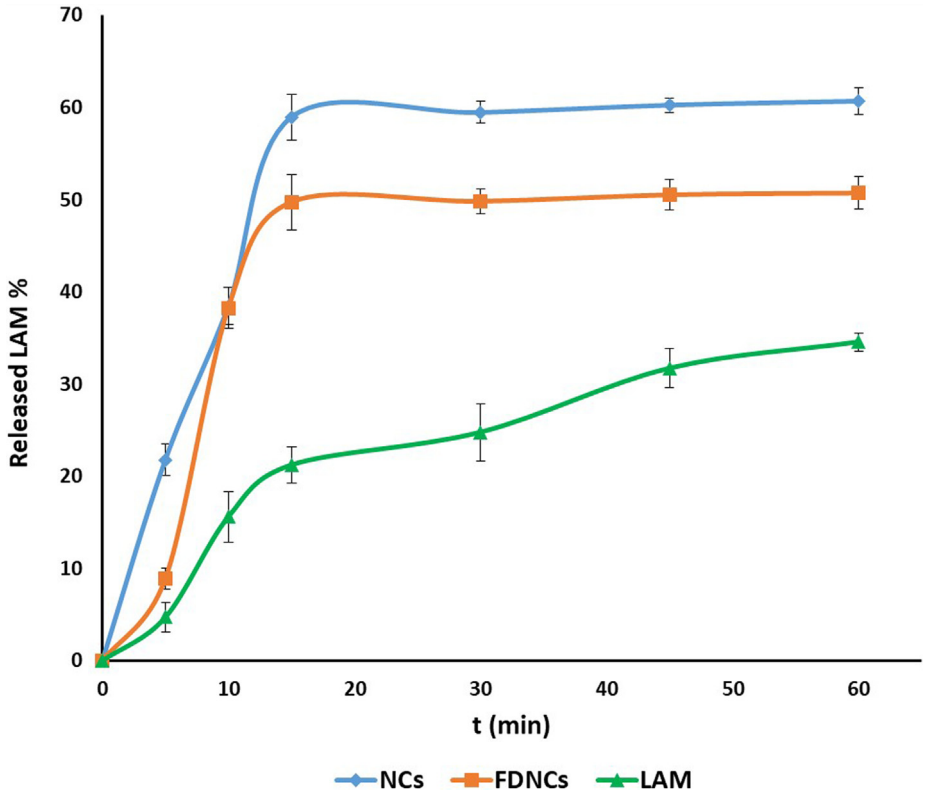

Fig. 4. *In vitro* drug release from different NCs formulations and LAM powder.

better than a LAM powder, which achieved the lowest amount of permeated drug. In the case of the NCs formulations ~25 µg/cm^2 LAM diffused through the cellulose ester membrane, which is 2.5 times higher than the amount of drug diffused from the raw powder formulation. This was a remarkably high amount if we take into consideration that an average human nasal mucosa is around 150–200 cm^2 [62].

Tha calculated Flux (J) and permeability coefficient (Kp) values (Table 3). The Flux shows how much API can diffuse through the membrane per hour and surface unit, while Kp is the Flux-donor phase ratio. The results of the table shows that tha LAM could diffuse in higher amount through the membrane to the acceptor phase from the NC formulations than from the powder, and that there was no significant difference between both nanoformulations. These results validated the previous observations on drug diffusion, as the NC formulations showed higher values for these parmaters than the powder. Compared to a previously reported, nanosized LAM containing nasal powder formualtion, the Flux is lower, but the permeability coefficient values predict good permeability through biological barriers [49].

3.7. *In vivo drug release study*

In a final step, we performed the *in vivo* administration of the LAM formulations and we performed PK analysis both in the brain and in the blood (Figs. 6 and 7, respectively). Nasal administration of LAM in NCs achieved higher brain drug concentrations than FDNCs. Also, the c_{max} of NCs was higher (0.23 µg/brain g) than after the administration of FDNCs (0.07 µg/brain g). The t_{max} was 60 min in the case of NCs, while it was 3 min when FDNCs were given to the rats. Indeed, NCs resulted in significantly higher AUC values (11.65 ± 1.03 min*µg/brain g) than FDNCs (2.06 ± 1.11 min*µg/brain g), while the AUC value of IV administration was 250.603 ± 7.66 min*µg/ brain g. The ratio of AUC values between the liquid and the solid NCs was 5.65, which means that this formulation was capable of providing better drug absorption. In any case, LAM was present in the CNS shortly after administration since it was detected there even at the 3 min extraction point. This time seems too short for LAM to be absorbed and to cross through the BBB, which indicates a possible axonal and paracellular transport of the drug [63]. Besides, in the case of FDNCs, the drug would take more time to be absorbed to the systemic circulation (Fig. 7.) through the nasal

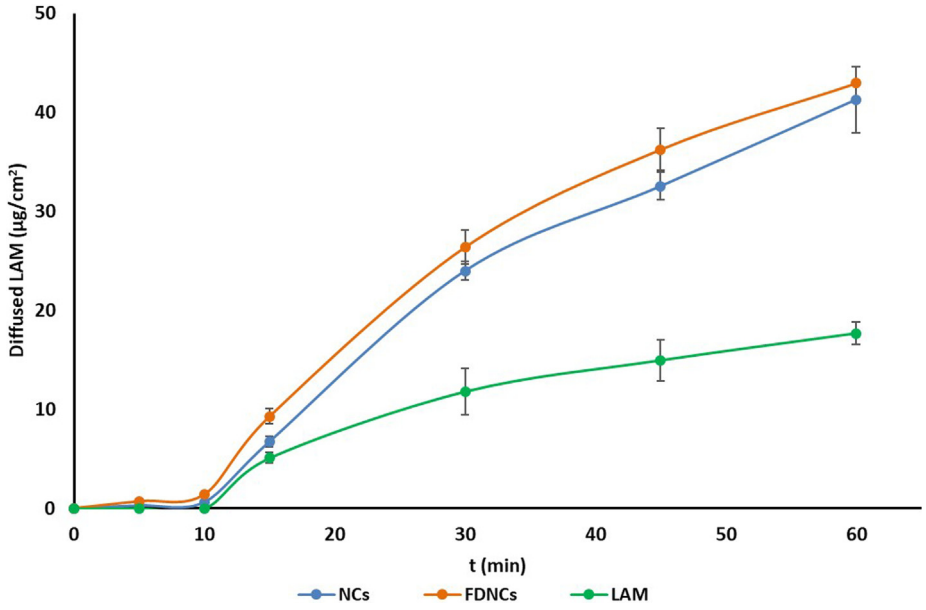

Fig. 5. *In vitro* permeability study of LAM in different formulations.

Table 3
Calculated Flux (J) and permeability coefficient (K_p) values for the different LAM formulations.

	J (µg/cm²/h)	K_p (cm/h)
LAM	35.29 ± 8.92	0.011 ± 0.002
NCs	41.29 ± 5.47	0.023 ± 0.005
FDNCs	42.96 ± 4.13	0.03 ± 0.005

mucosa, but it is still detected in the CNS. FDNCs showed very constant LAM levels in the CNS after the first 10 min, and we hypthesize that this could be due to the presence of parallel transport mechanism of axonal transport and access through the BBB.

We also determined the concentration of LAM in the blood plasma vs. time (Fig. 7). The plasma concentration of LAM was significantly higher for the NCs group than for the FDNCs group, an this was particularly remarkable in the 3 min datapoint: 0.18 ± 0.032 µg/mL vs. 0.01 ± 0.002 µg/mL LAM concentration for NCs and FDNCs, repectively. This could be explained by the fact that the API reached the systemic circulation without passing through the liver. Another possible explanation of the relatively high absorption of liquid NCs is that the liquid could spread over a larger surface that caused higher plasma concentrations. Moreover, another possible explanation of the poor permeation of the FDNCs is that in the nasal cavity the amount of water is limited. As the solid particles needs to be solubilized before permeation, this limited amount of water can retard or even limit the extent of the absorption. The ratio of AUC values shows that the API from the liquid NCs reached the plasma 12.28-fold more than the API in freeze-dried NCs ($AUC_{(NCs)}$ = 6.13 ± 0.52 min*µg/mL plasma; $AUC_{(FDNCs)}$ = 0.50 ± 0.16 min*µg/mL), but they were well below the IV formulation (125.08 ± 17.46 min*µg/mL). The c_{max} value was much higher (0.18 µg/mL) in the case of NCs, which was detected after 3 min (t_{max}) than it was in the case of FDNCs administration (0.14 µg/mL), which was detected after 10 min.

Table 4. represents the calculated values of the investigation. The brain:plasma ratios of the NCs and FDNCs were 1.90, and 4.13, respectively. This means that the API was more concentrated in the CNS than in blood plasma. The fact that this value is higher for the FDNCs than for the NCs indicates that this concentration ratio is not only dependent of drug biodistribution, but rather on other biopharmaceutical processes. We think that this higher ratio achieved with FDNCs could indicate a higher contribution of paracellular and direct axonal drug transport for this formulation as compared to NCs.

The cerebral drug targeting efficiency index (DTE) reflects the relative accumulation of the drug in the brain following intranasal

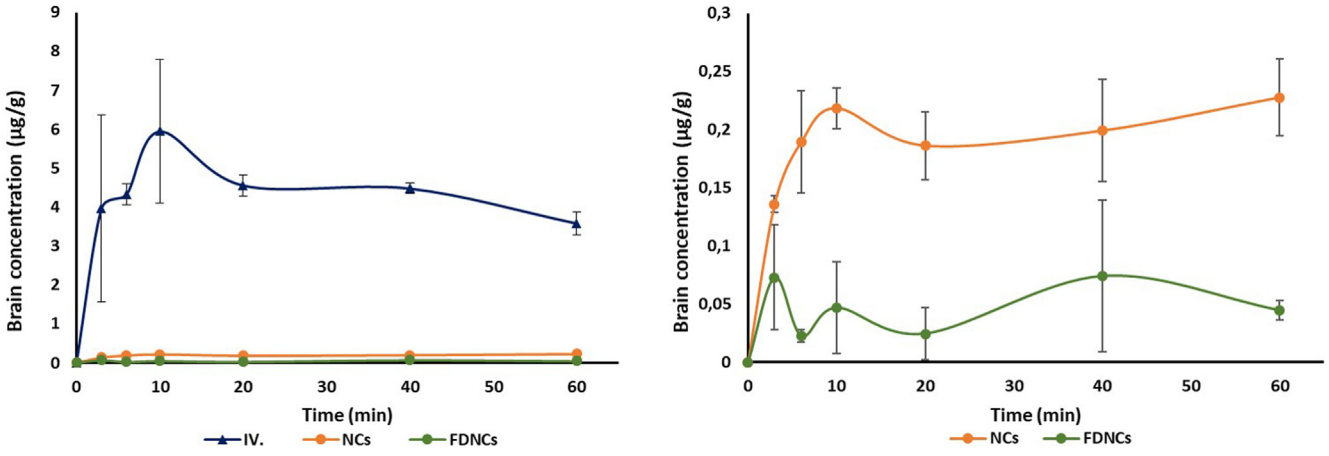

Fig. 6. The concentration values of LAM in the brain tissues.

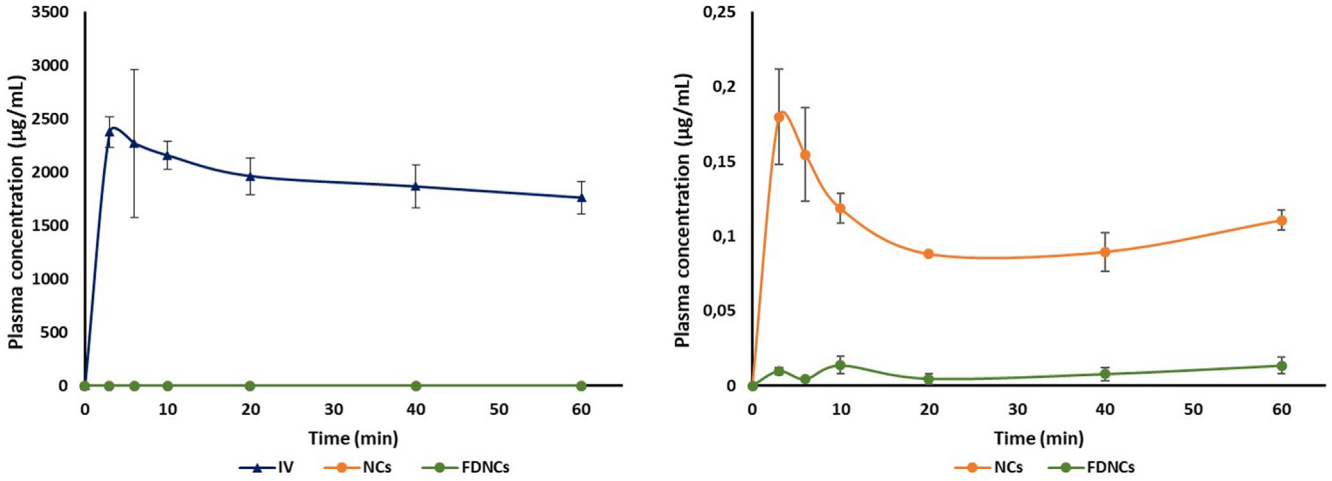

Fig. 7. The concentration values of LAM in the blood plasma.

Table 4
Calculated parameters of intranasal powders applying IV administration as a benchmark.

	AUC_{brain}/AUC_{blood}	DTE
IV injection	2.02	1
NCs	1.90	0.94
FDNCs	4.13	2.04

administration as compared to systemic administration. DTE data was around 1.0 in case of NCs, which means that LAM presented in similar concentrations in plasma and brain tissues, respectively. As for the FDNCs, the LAM could reach the brain tissues two times more efficiently via axonal transport, than through the systemic circulation, which is indicated by the value above 2.0. This resulted in remarkable absorption through the nasal mucosa directly into the CNS and parallelly resulted in poor transepithelial absorption into the systemic circulation in case of the solid state sample.

4. Conclusion

The aim of this study was to develop and investigate novel, LAM containing NCs. After preliminary experiments and size optimization, chitosan coated NCs with LAM were formulated both as a liquid suspension and as freeze-dried powder. The particle size of the NCs was always under 500 nm that meets with the particle size criteria of nanosystems according to regulatory guidelines and this nanosize was maintained after freeze-drying. The zeta potential was almost neutral in NCs, that could have a positive effect on mucoadhesion and mucodiffusion, and turned out to be positive in FDNCs, that could advantageous as in the blood stream, the particles could not be rapidly opsonized and cleared by macrophages. The encapsulation efficiency was acceptable, while the NCs were spherical and homogenous with no sign of aggregation in both samples. LAM was released quickly from both NCs formulations, with 50% payload released after 15 min, which predicted great release *in vivo*. The permeation rate of LAM was also higher for the NC samples than for LAM in powder form. *In vivo* studies showed that LAM could reach the brain in significant amounts, particulary for the liquid state NCs formulation that also showed remarkably high blood plasma levels of the API. The kinetics and biodistribution ratio of the drug between brain and plasma suggest that there is axonal transport involved in drug absorption, which means that the LAM can reach its site of action in an amount sufficient for effect. All in all it can be said, that the novel, NC formulation can offer a great alternative for LAM administration into the CNS in consdiderably high amount and with the use of this kind of nanoformulation the advantages of nanosystems and nasal delivery can be combined.

Acknowledgments

This project was supported by Gedeon Richter Ltd – GINOP project (2.2.1-15-2016-00007).

This project was supported by UNKP-19-3-SZTE-53 project.

This project was supported by Ministry of Human Capacities, Hungary grant 20391- 3/2018/FEKUSTRAT.

Declaration of Competing Interest

The authors declare that they have no known competing financial interests or personal relationships that could have appeared to influence the work reported in this paper.

References

[1] L.N. Thwala, D.P. Delgado, K. Leone, I. Marigo, F. Benetti, M. Chenlo, C.V. Alvarez, S. Tovar, C. Dieguez, N.S. Csaba, M.J. Alonso, Protamine nanocapsules as carriers for oral peptide delivery, J. Control. Release 291 (2018) 157–168, https://doi.org/10.1016/j.jconrel.2018.10.022.

[2] R.P. Moura, Lipid nanocapsules to enhance drug bioavailability to the central nervous system, J. Control. Release 11 (2020).

[3] K. Radhakrishnan, Stimuli-responsive protamine-based biodegradable nanocapsules for enhanced bioavailability and intracellular delivery of anticancer agents, J. Nanopart. Res. 12 (2015).

[4] P. Jakubiak, L.N. Thwala, A. Cadete, V. Préat, M.J. Alonso, A. Beloqui, N. Csaba, Solvent-free protamine nanocapsules as carriers for mucosal delivery of therapeutics, Eur. Polym. J. 93 (2017) 695–705, https://doi.org/10.1016/j.eurpolymj.2017.03.049.

[5] E. Borrajo, R. Abellan-Pose, A. Soto, M. Garcia-Fuentes, N. Csaba, M.J. Alonso, A. Vidal, Docetaxel-loaded polyglutamic acid-PEG nanocapsules for the treatment of metastatic cancer, J. Control. Release 238 (2016) 263–271, https://doi.org/10.1016/j.jconrel.2016.07.048.

[6] R. Abellan-Pose, M. Rodríguez-Évora, S. Vicente, N. Csaba, C. Évora, M.J. Alonso, A. Delgado, Biodistribution of radiolabeled polyglutamic acid and PEG-polyglutamic acid nanocapsules, Eur. J. Pharm. Biopharm. 112 (2017) 155–163, https://doi.org/10.1016/j.ejpb.2016.11.015.

[7] L.N. Thwala, A. Beloqui, N.S. Csaba, D. González-Touceda, S. Tovar, C. Dieguez, M.J. Alonso, V. Préat, The interaction of protamine nanocapsules with the intestinal epithelium: a mechanistic approach, J. Control. Release 243 (2016) 109–120, https://doi.org/10.1016/j.jconrel.2016.10.002.

[8] I. Santalices, D. Torres, M.V. Lozano, M.M. Arroyo-Jiménez, M.J. Alonso, M.J. Santander-Ortega, Influence of the surface properties of nanocapsules on their interaction with intestinal barriers, Eur. J. Pharm. Biopharm. 133 (2018) 203–213, https://doi.org/10.1016/j.ejpb.2018.09.023.

[9] J.V. González-Aramundiz, E. Presas, I. Dalmau-Mena, S. Martínez-Pulgarín, C. Alonso, J.M. Escribano, M.J. Alonso, N.S. Csaba, Rational design of protamine nanocapsules as antigen delivery carriers, J. Control. Release 245 (2017) 62–69, https://doi.org/10.1016/j.jconrel.2016.11.012.

[10] R. Abellan-Pose, C. Teijeiro-Valiño, M.J. Santander-Ortega, E. Borrajo, A. Vidal, M. Garcia-Fuentes, N. Csaba, M.J. Alonso, Polyaminoacid nanocapsules for drug delivery to the lymphatic system: effect of the particle size, Int. J. Pharm. 509

(2016) 107–117, https://doi.org/10.1016/j.ijpharm.2016.05.034.
[11] N. Csaba, M. Köping-Höggård, M.J. Alonso, Ionically crosslinked chitosan/tripolyphosphate nanoparticles for oligonucleotide and plasmid DNA delivery, Int. J. Pharm. 382 (2009) 205–214, https://doi.org/10.1016/j.ijpharm.2009.07.028.
[12] A. Beloqui, P.B. Memvanga, R. Coco, S. Reimondez-Troitiño, M. Alhouayek, G.G. Muccioli, M.J. Alonso, N. Csaba, M. de la Fuente, V. Préat, A comparative study of curcumin-loaded lipid-based nanocarriers in the treatment of inflammatory bowel disease, Colloids Surf., B 143 (2016) 327–335, https://doi.org/10.1016/j.colsurfb.2016.03.038.
[13] J.V. González-Aramundiz, M. Peleteiro Olmedo, Á. González-Fernández, M.J. Alonso Fernández, N.S. Csaba, Protamine-based nanoparticles as new antigen delivery systems, Eur. J. Pharm. Biopharm. 97 (2015) 51–59, https://doi.org/10.1016/j.ejpb.2015.09.019.
[14] G.R. Rivera-Rodriguez, G. Lollo, T. Montier, J.P. Benoit, C. Passirani, M.J. Alonso, D. Torres, In vivo evaluation of poly-l-asparagine nanocapsules as carriers for anticancer drug delivery, Int. J. Pharm. 458 (2013) 83–89, https://doi.org/10.1016/j.ijpharm.2013.09.038.
[15] J. Lademann, A. Patzelt, H. Richter, O. Lademann, G. Baier, L. Breucker, K. Landfester, Nanocapsules for drug delivery through the skin barrier by tissue-tolerable plasma, Laser Phys. Lett. 10 (2013) 083001, https://doi.org/10.1088/1612-2011/10/8/083001.
[16] M. Waykar, D.K.S. Salunkhe, D.M.J. Chavan, D.J.C. Hundiwale, K. Gite, S. Talke, A review on: nanocapsules, World J. Pharm. Pharm. Sci. 7 (n.d.) 10.
[17] C.E. Mora-Huertas, H. Fessi, A. Elaissari, Polymer-based nanocapsules for drug delivery, Int. J. Pharm. 385 (2010) 113–142, https://doi.org/10.1016/j.ijpharm.2009.10.018.
[18] S. Guterres, F. Poletto, L. Colom√©, R. Raffin, A. Pohlmann, Polymeric nanocapsules for drug delivery: an overview, in: M. Fanun (Ed.), Colloids in Drug Delivery, CRC Press, 2010, pp. 71–98. https://doi.org/10.1201/9781439818268-c3.
[19] F. Sonvico, A. Clementino, F. Buttini, G. Colombo, S. Pescina, S. Stanisçuaski Guterres, A. Raffin Pohlmann, S. Nicoli, Surface-modified nanocarriers for nose-to-brain delivery: from bioadhesion to targeting, Pharmaceutics 10 (2018) 34, https://doi.org/10.3390/pharmaceutics10010034.
[20] L. Kürti, R. Gáspár, Á. Márki, E. Kápolna, A. Bocsik, S. Veszelka, C. Bartos, R. Ambrus, M. Vastag, M.A. Deli, P. Szabó-Révész, In vitro and in vivo characterization of meloxicam nanoparticles designed for nasal administration, Eur. J. Pharm. Sci. 50 (2013) 86–92, https://doi.org/10.1016/j.ejps.2013.03.012.
[21] A. Mistry, S. Stolnik, L. Illum, Nanoparticles for direct nose-to-brain delivery of drugs, Int. J. Pharm. 379 (2009) 146–157, https://doi.org/10.1016/j.ijpharm.2009.06.019.
[22] S. Horvát, A. Fehér, H. Wolburg, P. Sipos, S. Veszelka, A. Tóth, L. Kis, A. Kurunczi, G. Balogh, L. Kürti, I. Erős, P. Szabó-Révész, M.A. Deli, Sodium hyaluronate as a mucoadhesive component in nasal formulation enhances delivery of molecules to brain tissue, Eur. J. Pharm. Biopharm. 72 (2009) 252–259, https://doi.org/10.1016/j.ejpb.2008.10.009.
[23] T. Horváth, R. Ambrus, G. Völgyi, M. Budai-Szűcs, Á. Márki, P. Sipos, C. Bartos, A.B. Seres, A. Sztojkov-Ivanov, K. Takács-Novák, E. Csányi, R. Gáspár, P. Szabó-Révész, Effect of solubility enhancement on nasal absorption of meloxicam, Eur. J. Pharm. Sci. 95 (2016) 96–102, https://doi.org/10.1016/j.ejps.2016.05.031.
[24] Z.N. Warnken, H.D.C. Smyth, A.B. Watts, S. Weitman, J.G. Kuhn, R.O. Williams, Formulation and device design to increase nose to brain drug delivery, J. Drug Delivery Sci. Technol. 35 (2016) 213–222, https://doi.org/10.1016/j.jddst.2016.05.003.
[25] C. Bartos, R. Ambrus, P. Sipos, M. Budai-Szűcs, E. Csányi, R. Gáspár, Á. Márki, A.B. Seres, A. Sztojkov-Ivanov, T. Horváth, P. Szabó-Révész, Study of sodium hyaluronate-based intranasal formulations containing micro- or nanosized meloxicam particles, Int. J. Pharm. 491 (2015) 198–207, https://doi.org/10.1016/j.ijpharm.2015.06.046.
[26] L. Nasare, K. Niranjane, A. Nagdevte, S. Mohril, Nasal drug delivery system: an emerging approach for brain targeting, World J. Pharm. Pharm. Sci. 3 (n.d.) 15.
[27] N. Csaba, M. Garcia-Fuentes, M.J. Alonso, Nanoparticles for nasal vaccination, Adv. Drug Deliv. Rev. 61 (2009) 140–157, https://doi.org/10.1016/j.addr.2008.09.005.
[28] R.P. Chen, From nose to brain: the promise of peptide therapy for Alzheimer's disease and other neurodegenerative diseases, J. Alzheimer's Disease Parkinsonism 07 (2017), https://doi.org/10.4172/2161-0460.1000314.
[29] Y.S.R. Elnaggar, S.M. Etman, D.A. Abdelmonsif, O.Y. Abdallah, Intranasal piperine-loaded chitosan nanoparticles as brain-targeted therapy in Alzheimer's disease: optimization biological efficacy, and potential toxicity, J. Pharm. Sci. 104 (2015) 3544–3556, https://doi.org/10.1002/jps.24557.
[30] M.R. Patel, R.B. Patel, K.K. Bhatt, B.G. Patel, R.V. Gaikwad, Paliperidone microemulsion for nose-to-brain targeted drug delivery system: pharmacodynamic and pharmacokinetic evaluation, Drug Delivery 23 (2016) 346–354, https://doi.org/10.3109/10717544.2014.914602.
[31] E. Gavini, G. Rassu, L. Ferraro, S. Beggiato, A. Alhalaweh, S. Velaga, N. Marchetti, P. Bandiera, P. Giunchedi, A. Dalpiaz, Influence of polymeric microcarriers on the in vivo intranasal uptake of an anti-migraine drug for brain targeting, Eur. J. Pharm. Biopharm. 83 (2013) 174–183, https://doi.org/10.1016/j.ejpb.2012.10.010.
[32] M. Yasir, U.V.S. Sara, Solid lipid nanoparticles for nose to brain delivery of haloperidol: in vitro drug release and pharmacokinetics evaluation, Acta Pharmaceutica Sinica B 4 (2014) 454–463, https://doi.org/10.1016/j.apsb.2014.10.005.
[33] E. Gavini, A. Hegge, G. Rassu, V. Sanna, C. Testa, G. Pirisino, J. Karlsen, P. Giunchedi, Nasal administration of Carbamazepine using chitosan microspheres: in vitro/in vivo studies, Int. J. Pharm. 307 (2006) 9–15, https://doi.org/10.1016/j.ijpharm.2005.09.013.
[34] A. Serralheiro, G. Alves, A. Fortuna, A. Falcão, Direct nose-to-brain delivery of lamotrigine following intranasal administration to mice, Int. J. Pharm. 490 (2015) 39–46, https://doi.org/10.1016/j.ijpharm.2015.05.021.
[35] H. Kublik, M.T. Vidgren, Nasal delivery systems and their effect on deposition and absorption, Adv. Drug Deliv. Rev. 29 (1998) 157–177, https://doi.org/10.1016/S0169-409X(97)00067-7.
[36] D. Sharma, D. Maheshwari, G. Philip, R. Rana, S. Bhatia, M. Singh, R. Gabrani, S.K. Sharma, J. Ali, R.K. Sharma, S. Dang, Formulation and optimization of polymeric nanoparticles for intranasal delivery of Lorazepam using box-Behnken design: in vitro and in vivo evaluation, BioMed Res. Int. 2014 (2014) 1–14, https://doi.org/10.1155/2014/156010.
[37] A. Clementino, M. Batger, G. Garrastazu, M. Pozzoli, E. Del Favero, V. Rondelli, B. Gutfilen, T. Barboza, M.B. Sukkar, S.A.L. Souza, L. Cantù, F. Sonvico, The nasal delivery of nanoencapsulated statins – an approach for brain delivery, Int. J. Nanomed. 11 (2016) 6575–6590, https://doi.org/10.2147/IJN.S119033.
[38] S. El-Safy, S.N. Tammam, M. Abdel-Halim, M.E. Ali, J. Youshia, M.A. Shetab Boushehri, A. Lamprecht, S. Mansour, Collagenase loaded chitosan nanoparticles for digestion of the collagenous scar in liver fibrosis: the effect of chitosan intrinsic collagen binding on the success of targeting, Eur. J. Pharm. Biopharm. 148 (2020) 54–66, https://doi.org/10.1016/j.ejpb.2020.01.003.
[39] W.R. Garnett, Lamotrigine: pharmacokinetics, J. Child Neurol. 12 (1997) S10–S15, https://doi.org/10.1177/088307389701201041.
[40] T. Alam, J. Pandit, D. Vohora, M. Aqil, A. Ali, Y. Sultana, Optimization of nanostructured lipid carriers of lamotrigine for brain delivery: *in vitro* characterization and *in vivo* efficacy in epilepsy, Expert Opin. Drug Del. 12 (2015) 181–194, https://doi.org/10.1517/17425247.2014.945416.
[41] J. Lalani, S. Patil, A. Kolate, R. Lalani, A. Misra, Protein-functionalized PLGA nanoparticles of lamotrigine for neuropathic pain management, AAPS PharmSciTech. 16 (2015) 413–427, https://doi.org/10.1208/s12249-014-0235-3.
[42] A.P. Rani, H. Veesam, Full factorial design in formulation of lamotrigine suspension using locust bean gum, Int. J. Chem. Sci. (2013) 10.
[43] S. Soltanpour, A. Jouyban, Solubility of lamotrigine in binary and ternary mixtures of N-methyl pyrrolidone and water with polyethylene glycols 200, 400, and 600 at 298.2K, J. Mol. Liq. 180 (2013) 1–6, https://doi.org/10.1016/j.molliq.2012.12.029.
[44] E.Y. Abu-Rish, S.Y. Elhayek, Y.S. Mohamed, I. Hamad, Y. Bustanji, Evaluation of immunomodulatory effects of lamotrigine in BALB/c mice, Acta Pharmaceutica. 67 (2017) 543–555, https://doi.org/10.1515/acph-2017-0035.
[45] E.Y. Abu-rish, L.A. Dahabiyeh, Y. Bustanji, Y.S. Mohamed, M.J. Browning, Effect of lamotrigine on in vivo and in vitro cytokine secretion in murine model of inflammation, J. Neuroimmunol. 322 (2018) 36–45, https://doi.org/10.1016/j.jneuroim.2018.06.008.
[46] H. Chen, S. Grover, L. Yu, G. Walker, A. Mutlib, Bioactivation of lamotrigine in vivo in rat and in vitro in human liver microsomes, hepatocytes, and epidermal keratinocytes: characterization of thioether conjugates by liquid chromatography/mass spectrometry and high field nuclear magnetic resonance spectroscopy, Chem. Res. Toxicol. 23 (2010) 159–170, https://doi.org/10.1021/tx9003243.
[47] G.V. Yadav, S.R. Singh, Gastroretentive drug delivery system of lamotrigine: in vivo evaluation, 6 (n.d.) 7.
[48] M. Wangemann, A. Retzow, B. Pohlmann-Eden, In vivo biopharmaceutical characterisation of a new formulation containing the antiepileptic drug lamotrigine in comparison to plain and dispersible/chewable lamotrigine tablets, Arzneimittelforschung 55 (2011) 307–311, https://doi.org/10.1055/s-0031-1296864.
[49] P. Gieszinger, I. Csóka, E. Pallagi, G. Katona, O. Jójárt-Laczkovich, P. Szabó-Révész, R. Ambrus, Preliminary study of nanonized lamotrigine containing products for nasal powder formulation, Drug Des. Dev. Ther. 11 (2017) 2453–2466, https://doi.org/10.2147/DDDT.S138559.
[50] P. Gieszinger, I. Tomuta, T. Casian, Cs. Bartos, P. Szabó-Révész, R. Ambrus, Definition and validation of the Design Space for co-milled nasal powder containing nanosized lamotrigine, Drug Dev. Ind. Pharm. 44 (2018) 1622–1630, https://doi.org/10.1080/03639045.2018.1483388.
[51] F. Sonvico, F. Zimetti, A.R. Pohlmann, S.S. Guterres, Drug delivery to the brain: how can nanoencapsulated statins be used in the clinic? Ther. Del. 8 (2017) 625–631, https://doi.org/10.4155/tde-2017-0044.
[52] F.N. Fonseca, A.H. Betti, F.C. Carvalho, M.P.D. Gremião, F.A. Dimer, S.S. Guterres, M.L. Tebaldi, S.M.K. Rates, A.R. Pohlmann, Mucoadhesive amphiphilic methacrylic copolymer-functionalized poly(< I > ε < /I > -caprolactone) nanocapsules for nose-to-brain delivery of olanzapine, J. Biomed. Nanotechnol. 11 (2015) 1472–1481, https://doi.org/10.1166/jbn.2015.2078.
[53] C. Prego, D. Torres, M.J. Alonso, Chitosan nanocapsules: a new carrier for nasal peptide delivery, J. Drug Del. Sci. Technol. 16 (2006) 331–337, https://doi.org/10.1016/S1773-2247(06)50061-9.
[54] K. Karimi, E. Pallagi, P. Szabó-Révész, I. Csóka, R. Ambrus, Development of a microparticle-based dry powder inhalation formulation of ciprofloxacin hydrochloride applying the quality by design approach, Drug Des. Dev. Ther. 10 (2016) 3331–3343, https://doi.org/10.2147/DDDT.S116443.
[55] L. Kozlovskaya, M. Abou-Kaoud, D. Stepensky, Quantitative analysis of drug delivery to the brain via nasal route, J. Control. Release 189 (2014) 133–140, https://doi.org/10.1016/j.jconrel.2014.06.053.
[56] Y. Zhang, M. Huo, J. Zhou, S. Xie, PKSolver: an add-in program for pharmacokinetic and pharmacodynamic data analysis in Microsoft Excel, Comput. Methods Programs Biomed. 99 (2010) 306–314, https://doi.org/10.1016/j.cmpb.2010.01.007.
[57] Guidance for industry considering whether an FDA-regulated product involves the application of nanotechnology, Biotechnol. Law Rep. 30 (2011) 613–616. https://

doi.org/10.1089/blr.2011.9814.
[58] L.M. Ensign, C. Schneider, J.S. Suk, R. Cone, J. Hanes, Mucus penetrating nanoparticles: biophysical tool and method of drug and gene delivery, Adv. Mater. 24 (2012) 3887–3894, https://doi.org/10.1002/adma.201201800.
[59] E. Marttin, N.G.M. Schipper, J.C. Verhoef, Nasal mucociliary clearance as a factor in nasal drug delivery, Adv. Drug Deliv. Rev. 26 (1998).
[60] M.I. Ugwoke, R.U. Agu, N. Verbeke, R. Kinget, Nasal mucoadhesive drug delivery: background, applications, trends and future perspectivesB, Adv. Drug Deliv. Rev. 26 (2005).
[61] L. Casettari, L. Illum, Chitosan in nasal delivery systems for therapeutic drugs, J. Control. Release 12 (2014).
[62] M. Kapoor, J.C. Cloyd, R.A. Siegel, A review of intranasal formulations for the treatment of seizure emergencies, J. Control. Release 237 (2016) 147–159, https://doi.org/10.1016/j.jconrel.2016.07.001.
[63] T.P. Crowe, M.H.W. Greenlee, A.G. Kanthasamy, W.H. Hsu, Mechanism of intranasal drug delivery directly to the brain, Life Sci. 195 (2018) 44–52, https://doi.org/10.1016/j.lfs.2017.12.025.